(American Metrological Society. In review)

The Arctic Ocean as a coupled oscillating system to the forced 18.6 year lunar gravity cycle

Harald Yndestad

Aalesund University College, hy@hials.no

Abstract. The Arctic Ocean is a substantial energy sink for the Earth's Northern Hemisphere. Future fluctuations in its energy budget will have a major influence on the Arctic climate. A wavelet spectrum analysis of an extensive historical Arctic data series concludes that we may be able to understand Arctic climate dynamics as an oscillation system coupled to the forced 18.6 yr lunar nodal gravity cycle. This paper presents the results from a wavelet spectrum analysis of the data series which included polar movement, Arctic ice extent and the inflow of North Atlantic Water to the Norwegian Sea. The investigation shows a correlation better than R=0.6 between the astronomic 18.6 yr lunar nodal gravity cycle and identified 18 yr dominant cycles in the data series. The identified 18 yr cycles has phase-reversals synchronized to a 74 yr sub-harmonic lunar nodal cycle.

1 Introduction

The cold Arctic Ocean acts as an energy sink that influences the climate. The sun is never high in the sky, and most of its energy is reflected back to space by snow and ice in the summer. Cooled Arctic water accumulates in circulating layers. The Arctic Ocean has four layers, all with different densities and circulation patterns: Arctic Surface Water, Atlantic Water, Deep Water, and Bottom Water. Atlantic Water from the Norwegian Sea enters the Eurasian Basin through the Fram Strait underneath the surface layer. At a level of about 200–900 m, it follows the continental slope east and north until it meets the Transpolar Drift, then returns to the Greenland Sea. Deep Water down to 2600 m from the Norwegian Sea is exchanged

between the Greenland Sea and the Eurasian Basin. Deep Water residence time in the Eurasian Basin is estimated to be about 75 years (Bonisch and Schlosser, 1995). An oscillation disturbance on the Arctic system may introduce an oscillating effect on Arctic climate.

Most of the changes in Arctic climate are influenced by inflow of North Atlantic Water. North Atlantic Water passes through the Faroe-Shetland Channel and into the Norwegian Sea. The current continues northward with an inflow to the Barents Sea and to the Arctic Ocean through the Fram Strait. The current circulates in the Arctic Ocean and influences the Arctic ice extent before it returns to the Greenland Sea. From the Greenland Sea, the cold water continues south with the East Greenland Current and the Labrador Current. East of Newfoundland, the cold current meets the warm Atlantic drift from the south, and some water returns to the northern Atlantic Ocean.

The North Atlantic Current has large fluctuations (Fig. 2), and it has been known for decades that this current has a major influence on the climate of northern Europe. A possible cause for the large temperature fluctuations in the North Atlantic Water is the tidal oscillations resulting from gravity effects between the earth, moon and sun (Yndestad, Turrell and Ozhigin 2004). A gravity effect between these three bodies results in a set of long orbital cycles that may introduce climate oscillations on the earth (Pettersson 1915; Currie 1984; Imbrie and Imbrie 1980; Satterley 1996; Yndestad 2006). An oscillating gravity effect on the climate fluctuations implies there may be a coupled oscillation between gravity cycles and Arctic climate. This study investigates the relationship between the astronomic 18.6 yr lunar nodal tide and the dominant cycles in polar motion, North Atlantic Water and Arctic ice extent. The investigation concludes that the Arctic climate variability can be thought of as an oscillator coupled to the forced 18.6 yr lunar nodal gravity cycle. This coupled Arctic oscillation has temporary harmonic cycles in which interference between cycles may introduce phase-reversals.

2 Materials and methods

The polar position data series (y-direction) is based on official data from the International Earth Rotation Service (IERS) and covers the years from 1846 until 2005. The time series can be found at: <http://hpiers.obspm.fr/eoppc/eop/eopc01/>. The time series contains 10 samples per year from 1846 to 1900, and 20 samples per year from 1900 to 2002, with the celestial pole offset represented in arc degrees.

North Atlantic Water is estimated within the core of the Slope Current on the Scottish side of the Faroe-Shetland Channel where the temperature and salinity at the standard depth show a maximum salinity (Turrell et al. 1999). The data series covers 1893 to 2002 and has no values in the periods from 1895 to 1902, 1915 to 1922, 1930 to 1933, and 1941 to 1946. In these periods the data are cubic spline interpolated. The data series is provided by the FRS Marine Laboratory, Aberdeen (Turrell, personal communication).

The Arctic ice extent data series represents the sum of the Greenland Sea and Barents Sea ice extents. The area of the Greenland Sea ice extent discussed in this paper covers the Greenland Sea, the Iceland Sea and the Norwegian Sea bounded by 30°W, 10°E and 80°N. The data are based on values taken in April from 1850 until 2000. The Barents Sea ice extent covers the Norwegian Sea, the Barents Sea and the Kara Sea bounded by 10°E, 80°N and 70°E. The data are based on values from April between 1850 and 2000 (Vinje 2001). The coupled oscillating system may be represented by the simple system model

$$S(t) = \{B(t), \{S_s(t), S_m(t), S_e(t)\}\} \quad , \tag{1}$$

where $S_s(t)$ represents the sun system, $S_m(t)$ the moon system, $S_e(t)$ the earth system and B(t) the mutual gravity relation between the planetary systems. The mutual relation has a set of long-term cycles that may influence dynamics on the earth system. The 18.6 yr lunar nodal amplitude cycle and the 18.6/2=9.3 yr lunar nodal phase cycle are both important gravity cycles. The astronomic lunar nodal amplitude cycle period of T=18.6134 years introduces a periodic tide that has both vertical and horizontal components. The vertical component has a global influence on sea level and its greatest influence is at the Equator and at the Arctic Ocean, while it has a minimal influence at about 30 degrees from the Equator. The 18.6 yr amplitude tide has a maximum in November 1987, which represents a phase delay of about $\varphi_T(t)=0.90\pi$ rad in Eq. 3. The vertical tide causes a horizontal current component that has a phase angle of about $\varphi_T(t)=(0.90\text{-}0.50)\pi$ rad. The 9.3 yr lunar nodal cycle phase tide has a period of $T/2$=9.3 years and a phase-angle of about $\varphi_{T/2}(t)=1.41\pi$ rad (Pugh 1996).

In this analysis, the lunar nodal gravity cycles represents a stable long-term forced oscillation on the coupled earth system [$S_e(t)$]. The coupled earth system is expected to respond by a chain of reactions related to the movement of the earth's axis, earth mantle dynamics and tidal oscillation in the sea systems. A lunar nodal tide influence on circulating water may be modelled by the state model:

$$x(t) = a \cdot x(t-\tau) + u(t) \, , \tag{2}$$

where u(t) represents the tidal input to the circulation, x(t) the state at the time t, τ the ocean circulation delay and a the circulation temperature loss. Energy from a forced oscillating lunar nodal tide into a positive circulating water feedback system, will cause energy to be accumulated in a set of sub-harmonic cycles:

$$x(t) = \sum_k a_k(t)\sin(k\omega_T t + \varphi_{kT}(t)) + v(t) \quad , \qquad (3)$$

where $v(t)$ is a disturbance from an unknown source, $a_k(t)$ represents the cycle amplitude, $\omega_T=2\pi/T$ (rad y^{-1}) the cycle period, and $\varphi_{kT}(t)$ is the time-dependent phase angle. A cycle number k may have values k=1,2,3… on harmonic cycles and k=1/2,1/3… on sub-harmonic cycles in the lunar nodal spectrum, as evaluated for times t=1900,1901,…,2005. The long-term analysis was based on the assumption there is a possible 74 yr sub-harmonic cycle in the Arctic data series where the identified phase angle is $\varphi_{4T}(t)=0.29\pi$ rad (Yndestad 2006). A sub-harmonic cycle $a_{kT}(t)\sin(\omega_{kT}t)$ may have accumulated an amplitude $a_{kT}(t) >> a_T(t)$. This may introduce a phase-reversal in the forced lunar nodal cycle $a_{kT}(t)\sin(\omega_{kT}t)$ by interference. This investigation identified a phase-reversal in the 18.6 yr lunar nodal cycle which is related to the 74 yr sub-harmonic cycle.

Phase-reversals in the cycle periods introduce a time-variant stochastic process. This property excludes traditional spectrum analysis methods to identify cycle periods and cycle phase. In this study, the time-series have been analyzed by wavelet transformation to identify the dominant cycle periods $u_k(t)$ and the time-variant phase angle $\varphi_{kT}(t)$. The periodicity was identified by a three-step investigation. The first step was to compute the wavelet spectrum by the transformation:

$$W_{a,b}(t) = \frac{1}{\sqrt{a}}\int_R x(t)\Psi(\tfrac{t-b}{a})\mathrm{d}t \quad , \qquad (4)$$

where $x(t)$ is the time-series analyzed, and $\Psi(\,)$ is a coiflet wavelet impulse function (Daubechies 1992; Matlab 1997). $W_{a,b}(t)$ is a set of wavelet cycles, b is the translation in time, and a is the time-scaling parameter in wavelet transformation. The relationship between the wavelet scaling (a) and the sinus period T is about $T\approx 1.2a$. In this analysis, the translation b=0, so the computed wavelet transformation $W_a(t)$ represents a moving correlation between $x(t)$ and the impulse function $\Psi(\,)$ over the whole time-series $x(t)$.

Using this wavelet transformation, it is possible to identify single, long-period cycles in a short time-series. Errors at the beginning and at the end of a time-series are reduced in the following manner. The time-series are scaled in amplitude and to

the zero mean value by the scaling transformation $y(t)=[x(t)–\text{mean}(x(t))]/\text{var}(x(t))$, where $x(t)$ is the time-series, and $y(t)$ is the scaled time-series. Subsequently, the time-series is expanded with symmetric values at the beginning and end of the time-series. The cycle periods of single dominant-wavelet cycles are identified by computing the autocorrelation for the wavelet spectrum $R_w(\tau)=E[W_a(t)W_a(t+\tau)]$. Dominant, stationary wavelet cycles have maximum values in the autocorrelation functions. Periodic cycles in the autocorrelation function of the wavelet spectrum demonstrate that there is a stationary cycle. The cycle period phase is identified by the optimum correlation between dominant wavelets and lunar nodal cycles by $R_{kT}(\tau)=E[W_{ak}(t)u_{kT}(t)]$, where $u_{kT}(t)$ is a kT lunar nodal cycle period and the phase angle $\varphi_{kT}(t)$ is a free variable.

3 Results

3.1 Polar position

The pole position was influenced by the constellation between the earth, sun and the moon. The position changed in the y-direction from about 0.1 to 0.3 arc degrees, representing a displacement of approximately 5 to 15 meters. A computed wavelet spectrum from the polar position time series had dominant cycles with periods of about 1.2, 6, 18 and 74 years (Fig. 1). The correlations with the lunar nodal harmonic cycles of 18.6/3=6.3, 18.6 and 18.6*4=74.4 were estimated, with $R_{T/3}=0.44$, $R_T=0.7$ and $R_{4T}=0.86$ (Yndestad 2006). The 1.2 yr (Chandler wave) was most likely a 5 harmonic cycle from the forced 6.2 yr nodal cycle.

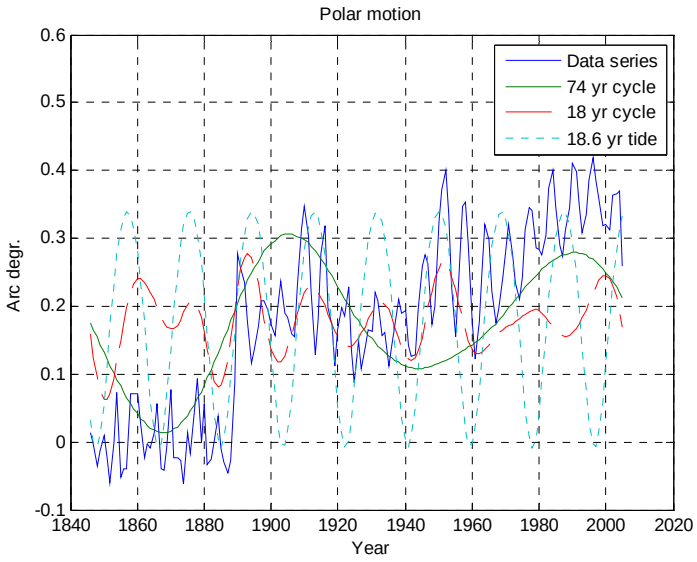

Figure 1. Polar motion in the y-direction relative to the dominant 18 yr wavelet cycle, the 18.6 yr lunar nodal tide cycle and the dominant 74 yr wavelet cycle.

The dominant 18 yr cycle had an estimated phase angle [$\varphi_{18}(t)$] of 0.90π rad between 1850 and 1960, which is the same as the lunar nodal cycle. After approximately 1960, the 18 yr cycle showed a phase-reversal. The dominant 74 yr wavelet cycle was at a minimum at about 1970 and 1940 and at a maximum at about 1910 and 1990, and turning points were observed at about 1890 and 1925. The phase-reversal of the 18 yr cycle introduced a phase delay of about 18.6/2 years and the next turning point was in 1970. The cycle phase angle was estimated to be $\varphi_{74}(t)$=1.29π rad.

3.2 North Atlantic Water

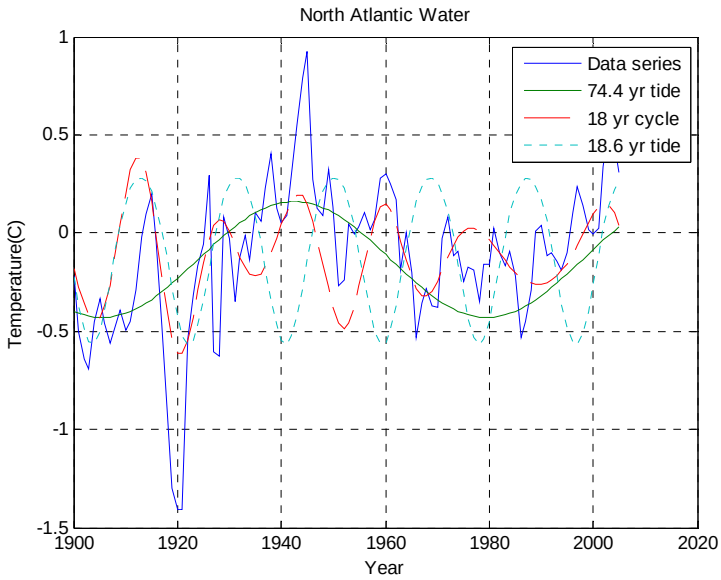

Figure 2. NAW temperature data series shown alongside the 74 yr harmonic lunar nodal tide, the identified 18 yr wavelet cycle, and the astronomic 18.6 yr lunar nodal tide cycle.

Figure 2 shows the time-series of the North Atlantic Water temperature on the Scotland side of the Faroe-Shetland Channel from 1900 to 2005 and represents one of the longest oceanographic time-series in the world. The data series demonstrates that the temperature has large fluctuations within a period of one hundred years. A wavelet analysis of the data series identified dominant cycles correlated with lunar nodal cycles of about 9, 18 and 74 years (Fig. 2). The dominant lunar nodal cycle periods was correlated with the astronomic lunar nodal tides, but had an unstable phase. The identified 74 yr wavelet cycle, $W_{74}(t)$, had an estimated phase of about $\varphi_{74}(t)=(0.29-0.10)\pi$ rad and represents the long-term mean temperature fluctuation. The 74 yr cycle had a reversed phase compared to the 74 yr polar movement cycle. The estimated phase of the identified 18 yr wavelet cycle $W_{18}(t)$ was about $\varphi_{18}(t)=0.90\pi$ rad for the period from 1900 to 1925, the same phase angle as the lunar nodal tide. At about 1925 the 74 yr period in polar movement changed to a negative state, the Atlantic water temperature changed to a positive state and the 18 yr cycle

had a phase-reversal from 1925 to 2004. In this period the correlation to the astronomic 18.6 yr lunar tide was estimated to be R_T=-0.68.

3.3 Arctic ice extent

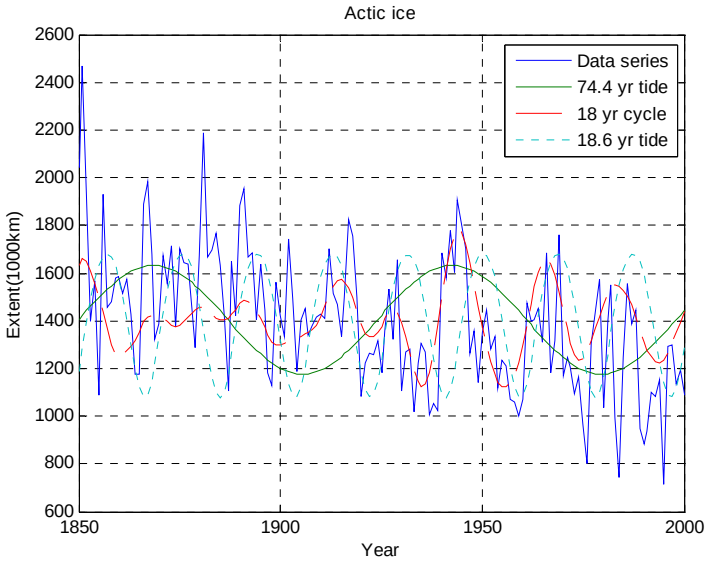

Figure 3. The Arctic ice extent data series in relation to the 74 yr harmonic lunar nodal tide, the identified 18 yr wavelet cycle and the astronomic 18.6 yr lunar nodal tide cycle.

A wavelet analysis of the Arctic ice extent data series identified the same dominant cycles of about 18 and 74 years as identified in the Polar motion data series and the North Atlantic Water. The dominant lunar nodal cycle periods were correlated with the astronomic lunar nodal tides, but had an unstable phase. The identified 74 yr wavelet cycle, $W_{74}(t)$, had a correlation of R_{4T}=0.91 with the 74.4 yr lunar nodal cycle and an estimated phase, $\varphi_{74}(t)$, of (0.29-0.18)π rad, representing a delay of about 7 years.

The identified 18 yr wavelet cycle, $W_{18}(t)$, had an estimated phase of about $\varphi_{18}(t)$=(0.90+0.5)π rad and R_T=0.4 during the period from 1850 to about 1925 when

the 74 yr cycle was becoming positive. From about 1925 to 2000 the 18 yr cycle had a phase-reversal and changed to the phase $\varphi_{18}(t)=(0.90-0.5)\pi$ rad. In this period the correlation to the astronomic 18.6 yr lunar tide was estimated to be $R_T=0.84$. The phase delay of 0.5π rad corresponded to the lunar nodal cycle current and could be explained by a delay in the circulation of Arctic water.

4 Discussion

The influence of the lunar nodal tide on climate has been discussed since the work of G. H. Darwin (1880) and Pettersson (1915). Russian scientists investigated this relationship up to the 1960's (Maksimov and Smirnov 1965, 1967). Currie (1987) identified the lunar nodal cycle in a number data series, and Keeling and Worf (1997) predicted a set of strong 18-yr tidal waves in the Atlantic Ocean. The lunar nodal tide represents only about 5% of the daily diurnal tide from the moon. A small lunar nodal tide has, however, much power when integrated in time and space over a period of 9 years. The introduction of wavelet spectrum analysis has made it possible to identify the phase-relation between dominant lunar cycles in data series from Atlantic sea level, North Atlantic temperature and salinity, Arctic ice extent, and the NAO-winter index (Yndestad, Turrell and Ozhigin 2004; Yndestad 2006). By comparing the cycle phases it is possible to understand the dynamics behind the chain of events.

This paper has focused on the close relationship between the identification of the lunar nodal cycle period, phase and phase-reversals in long Arctic climate data series. The investigation shows that polar motion, North Atlantic Water temperature and Arctic ice have dominant fluctuations and have a correlation better than R=0.68 with the astronomic 18.6 yr lunar nodal cycle. The exception is the first part of the Arctic ice data when there were unreliable observations (Vinje 2001). The long-term fluctuations were correlated with a sub-harmonic cycle of 18.6*4=74. 4 years. The North Atlantic Water 74 yr cycle had the same phase as the 74 yr cycle of Arctic ice extent. More Arctic ice and more Atlantic inflow indicate that the fluctuation had a phase-delay of about 74/2 years. The 74 yr cycle of polar motion had a phase delay of 1.0π rad or 74/2 years. The mean Arctic ice extent has been decreasing since about 1825 when ice extent was maximal. This indicates that longer sub-harmonic cycles influencing climate fluctuations may exist. The 18.6 yr periodic cycles had phase-reversals at about 1925 and 1960 when the 74 yr sub-harmonic cycle shifted in a new

direction. This phase-reversal explains why the lunar nodal spectrum has been difficult to identify by traditional spectrum analysis methods.

5. Conclusions

The wavelet analysis identified dominant cycles correlated with the 18.6 yr lunar nodal gravity cycle in Polar movement, North Atlantic Water and Arctic ice extent. The synchronization of cycle periods and phase indicates that the Arctic Ocean system oscillations are coupled to the forced 18.6 yr gravity cycle of the moon. The phase-reversals in the 18 yr tide is explained by interference between a 74 yr subharmonic cycle and the shorter 18 yr cycle. This phase-reversal property introduces a temporary time-variant system that may be understood as chaotic behaviour. The implication of a coupled Arctic oscillation system is that dominant climate fluctuations over the last 150 years may be explained by a gravity oscillation disturbance from the moon.

References

Bonisch, G and Schlosser, P. 1995. Deep water formation and exchange rates in the Greenland/Norwegian Seas and the Eurasian Bain of the Arctic Ocean derived from tracer balances. Prog. Oceanography. 35:29-52.

Currie, R. G.1984. Evidence for 18.6 year (*sic*) lunar nodal (*sic*) drought in western North America during the past millennium: Journal of Geophysical Research.89:1295-1308.

Currie, R. G. 1987. Examples and implications of 18.6- and 11--year terms in world weather records, Chap. 22, p. 378-403 *in* M.R. Rampino, J.E. Sanders, W.S. Newman,and L.K. Konigsson, *eds*. Climate: History, periodicity, and predictability: International Symposium held at Barnard College, Columbia University, New York, New York, 21-23 May 1984 (R. W. Fairbridge Festschrift): New York, NY, Van Nostrand Reinhold Publishing Corp., 588 p.

Darwin, G.H. 1880. On the secular change of the orbit of a satellite revolving about a tidally distorted planet. Philosophical Transactions of the Royal Society of London. 171: 713-891.

Daubechies I. 1992. Ten lectures of wavelet. SIAM Journal on Mathematical Analysis. 24:499-519.

Imbrie John, Imbrie John Z. 1980. Modeling the Climate response to Orbital Variations. Science. 207, 29 February 1980.

Keeling, Charles D. and T. P. Whorf. 1997. Possible forcing global temperature by oceanic tides. Proceedings, National Academy of Sciences of the United States. 94:8321-8328.

Maksimov, I. V. and N.P. Smirnov. 1965. A contribution to the study of causes of long-period variations in the activity of the Gulf Stream. Oceanology. 5:15-24.

Maksimov, I. V. and N.P. Smirnov. 1967. A long-term circumpolar tide and its significance for the circulation of ocean and atmosphere. Oceanology 7: 173-178.

Matlab. 1997. Matlab. Wavelet Toolbox. Users Guide. The Math Works Inc.

Pettersson, Otto, 1915, Long periodical (*sic*) variations of the tide-generating force: Conseil Permanente International pour l'Exploration de la Mer (Copenhagen), Pub. Circ. No. 65, p. 2-23.

Pugh, D T. 1996. Tides, Surges and Mean Sea-Level. John Wiley & Sons. New York.

Satterley, A. K. 1996. The Milankovitch Theory. Earth-Science Reviews. 40:181-207.

Turrell, WR, Sherwin, TJ, Jeans, DRG, et al. 1999. Eddies and mesoscale deflection of the slope current in the Faroe-Shetland Channel. DEEP-SEA RESEARCH PT I 46(3):415-438 MAR 1999.

Vinje, Torgny. 2001. Anomalies and trends of sea ice extent and atmospheric circulation in the Nordic Seas during the period 1864-1998. Journal of Climate. 14:255-267.

Yndestad H, Turrell W R, Ozhigin V. 2004. Temporal linkages between the Faroe-Shetland time series and the Kola section time series. ICES Annual Science Conference. Sept 2004. Vigo. ICES CM 2004/M.

Yndestad, H: 2006. The influence of the lunar nodal cycle on Arctic climate. Journal of Marine Science. 63. 401-420.